

# Supplementary Material

## Centimeter scale color printing with grayscale lithography

**Yu Chen,<sup>a,†</sup> Yang Li,<sup>a,†</sup> Wenhao Tang,<sup>a,†</sup> Yutao Tang,<sup>a</sup> Yue Hu,<sup>a</sup> Zixian Hu,<sup>a</sup> Junhong Deng,<sup>b</sup> Kokwai Cheah,<sup>c</sup> and Guixin Li<sup>a,\*</sup>**

<sup>a</sup>Department of Materials Science and Engineering, Southern University of Science and Technology, Shenzhen, 518055, China

<sup>b</sup>Shenzhen Institute for Quantum Science and Engineering, Southern University of Science and Technology, Shenzhen, 518055, China

<sup>c</sup>Department of Physics and Institute of Advanced Materials, Hong Kong Baptist University, Hong Kong, China

## Table of Contents

S1. The complex refractive index of the materials used in the simulation .....	2
S2. Numerical simulations of the Fabry-Perot cavities .....	3
S3. Optical measurements.....	4
S4. Measured and calculated transmission spectra of the color palettes .....	6
S5. Mapping transmission color to the CIE 1931 chromaticity diagram.....	7
S6. Design and fabrication of the color printing devices.....	9
S7. Color filter arrays based on the pixelated Fabry-Perot cavities.....	11

## **S1. The complex refractive index of the materials used in the simulation**

Figure S1(a), (b) and (c) show the complex refractive indexes of the used in designing the Fabry-Perot cavities. The black solid lines and red dashed lines represent the real part  $n$  and the imaginary part  $k$  of silver, photoresist and SiO<sub>2</sub> layers, respectively.

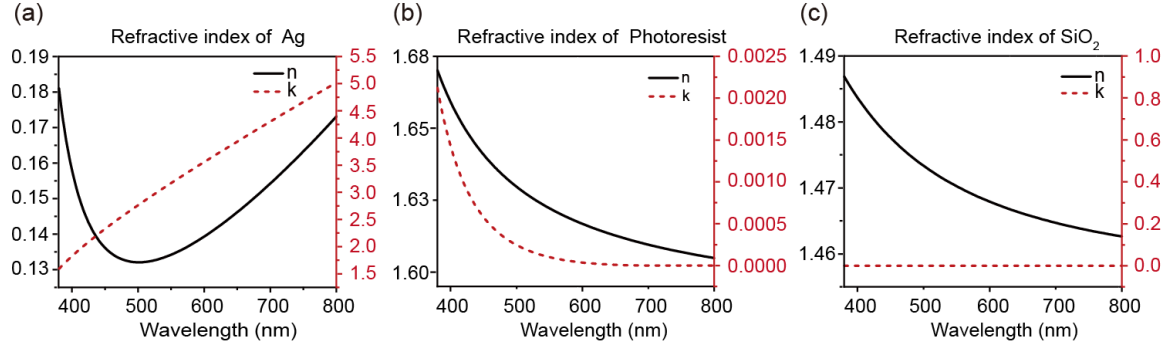


**Fig. S1** The measured refractive indexes of the materials used in designing the Fabry-Perot cavities. (a)–(c) The complex refractive index of Silver, photoresist and SiO<sub>2</sub> layer, respectively.

The complex refractive index of silver (Fig. S1(a)) is calculated from the Lorentz-Drude model.<sup>36</sup> The relative permittivity of silver can be expressed as a function of the angular frequency of the incident electromagnetic field,

$$\varepsilon_r(\omega) = 1 - \frac{f_0 \omega_p^2}{\omega(\omega - i\Gamma_0)} + \sum_{j=1}^m \frac{f_j \omega_p^2}{(\omega_j^2 - \omega^2) + i\omega\Gamma_j} \quad (\text{S1})$$

Where  $\omega_p$  is the plasma frequency,  $m$  is the number of oscillators with frequency  $\omega_j$ , strength  $f_j$  and damping constant  $\Gamma_j$ . The refractive indexes of the photoresist AZ 4562 (Fig. S1(b)) and the SiO<sub>2</sub> layer (Fig. S1(c)) were measured by using spectroscopic ellipsometry.

## **S2. Numerical simulations of the Fabry-Perot cavities**

The numerical simulations of the optical properties of the Fabry-Perot cavities were carried out by using the commercial software Lumerical FDTD Solutions. Based on the configuration of the F-P cavity in Fig. 2(a), a three-dimensional model was built to calculate the optical transmission spectra. We applied the periodic boundary condition in both  $x$  and  $y$  directions. Perfectly matched layer (PML) boundary condition was adopted in  $z$  direction. To save the calculation time, the period was set as  $1.0\ \mu\text{m}$  in both  $x$  and  $y$  directions. Mesh size was set as  $50.0\ \text{nm}$  in  $x$  and  $y$  directions and  $1.0\ \text{nm}$  in  $z$  direction. The calculated results are shown in both Fig. 2(b), (c) in the main text and Fig. S5(c).

### **S3. Optical measurements**

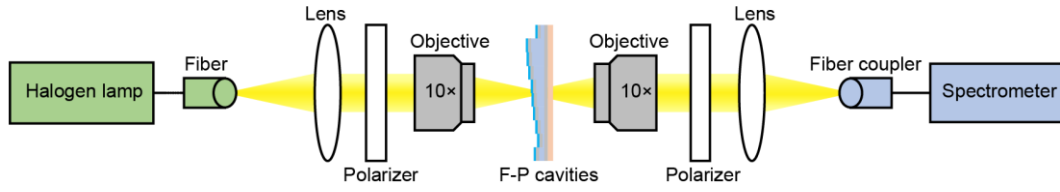


**Fig. S2** The optical setup for measuring the transmission spectra of the Fabry-Perot cavities.

The transmission spectra of the Fabry-Perot cavities were measured by using a home-made optical setup shown in Fig. S2. The fiber coupled white light from the halogen lamp is firstly collimated by Lens 1 and then polarized by the linear polarizer. After passing through a 10× objective lens, the incident light is normally incident on the Fabry-Perot cavities. The transmitted light is collected by the second objective lens and analyzer by the second polarizer. Finally, the transmission spectra can be obtained by using an Ocean optics spectrometer (USB 4000).

As shown in Fig. S3, the white balanced photos of the F-P cavities were captured by a Canon EOS RP camera with Canon lens (RF35mm F1.8 MACRO IS STM). For the photos in Fig. 4b, the exposure time of 1/1000 s, the aperture of f/1.8 and the ISO value of 400 were used in the camera setting.

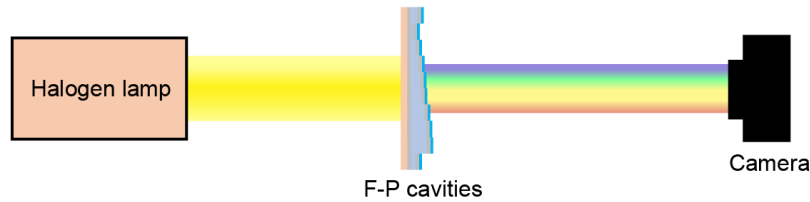


**Fig. S3** The optical setup for imaging of the Fabry-Perot cavities.

As shown in Fig. 4, we used a Zeiss microscope (Axion Observer) and the colorful digital camera (Axiocam 105 color) to observe the fine structures of the color printing device. A 5× objective lens was used to capture the images which are shown in Fig. S4(a) and Fig. 4(c), (d) in the main text. The microscopy images in Fig. 5 in the main text was captured by using the 20× objective lens.

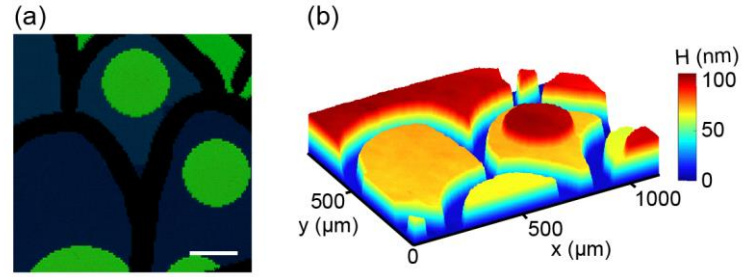


**Fig. S4** Magnified images of the pixelated Fabry-Perot cavities. (a) The microscopy image of green color F-P cavities. Scale bar: 200  $\mu\text{m}$ . (b) The 3D profile of a specific region of the color printing device. The profile was measured by using white light interferometer (Bruker Contour GTK0).

#### S4. Measured and calculated transmission spectra of the color palettes

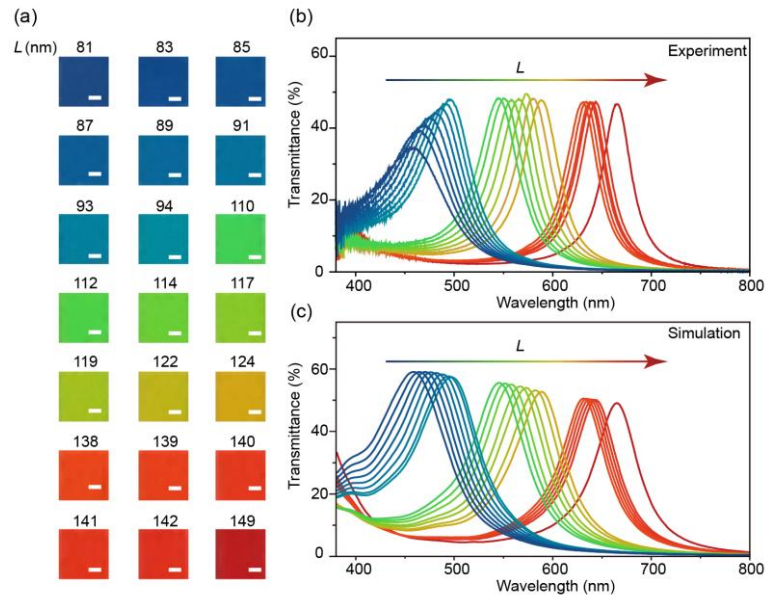


**Fig. S5** Optical properties of the F-P type color palettes. (a) White balanced photos of the color palettes, and  $L$  represents the retrieved effective thickness of the PR layer. The scale bar is 50  $\mu\text{m}$ . (b), (c) The measured and calculated transmission spectra of the color palettes.

Fig. S5(a) shows the photos of the color palettes taken by the Canon camera; each palette has an area of  $200 \times 200 \mu\text{m}^2$ . The retrieved thickness  $L$  of the photoresist are obtained by matching the measured transmission peaks with the calculated ones. Fig. S5(b), (c) are measured and calculated transmission spectra of the F-P type color palettes. By comparing (b) and (c) panels, it is clear that the simulation results qualitatively agree with the experimental ones.

## **S5. Mapping transmission color to the CIE 1931 chromaticity diagram**

The CIE chromaticity diagram is a standard method to evaluate the color from a light source or an object. Data points in the chromaticity diagram are related to tristimulus values  $X$ ,  $Y$  and  $Z$ . Colors can be quantized by the tristimulus values with the following equations (S2) – (S4):

$$X = K \int \bar{x}(\lambda) \cdot S(\lambda) \cdot T(\lambda) d\lambda \quad (\text{S2})$$

$$Y = K \int \bar{y}(\lambda) \cdot S(\lambda) \cdot T(\lambda) d\lambda \quad (\text{S3})$$

$$Z = K \int \bar{z}(\lambda) \cdot S(\lambda) \cdot T(\lambda) d\lambda \quad (\text{S4})$$

Where  $K$  is a scaling factor,  $\bar{x}(\lambda)$ ,  $\bar{y}(\lambda)$  and  $\bar{z}(\lambda)$  are color-matching functions which are related to the optical responses of human eyes. In transmission mode,  $S(\lambda)$  is the relative power of a light source,  $T(\lambda)$  is the transmission spectrum.

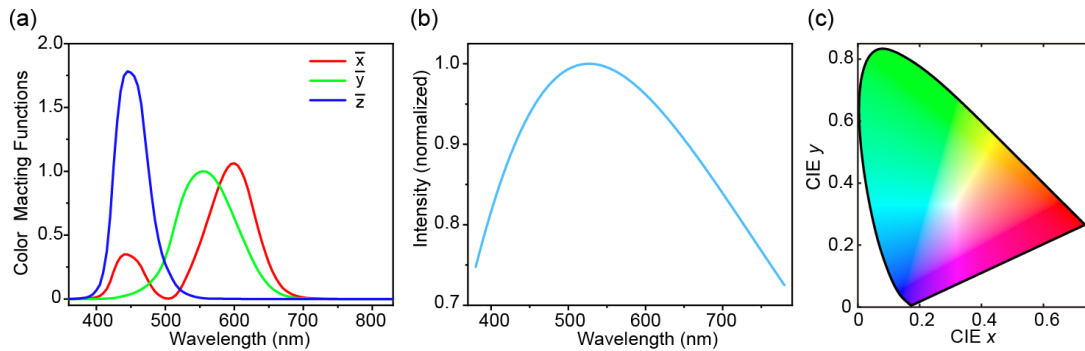


**Fig. S6** The details for calculating CIE chromaticity diagram. (a) The CIE 1931 color matching functions. (b) The normalized black-body radiation spectrum at  $T=5500\text{K}$ . (c) The CIE chromaticity diagram.

As shown in Fig. S6, we choose the CIE 1931 standard colorimetric observer as the color-matching functions with data from ISO/CIE 11664-1:2019. It is worth pointing out that the data points in the CIE  $xyY$  color space are normalized tristimulus values. The normalization method is illustrated in Equation (S5) – (S7). Due to the normalization, the brightness information of the color is missing, hence the CIE  $xyY$  color space only show the color hue and color saturation.

$$x = X / (X + Y + Z) \quad (\text{S5})$$

$$y = Y / (X + Y + Z) \quad (\text{S6})$$

$$z = 1 - x - y \quad (\text{S7})$$

The chromatic coordinates can be calculated by normalizing the color matching

functions,<sup>37</sup> as shown in Equation (S8) – (S10):

$$x_{coord.} = \bar{x} / (\bar{x} + \bar{y} + \bar{z}) \quad (S8)$$

$$y_{coord.} = \bar{y} / (\bar{x} + \bar{y} + \bar{z}) \quad (S9)$$

$$z_{coord.} = \bar{z} / (\bar{x} + \bar{y} + \bar{z}) \quad (S10)$$

The CIE chromatic diagram can be calculated according to the assumptions that  $x = X$ ,  $y = Y$  and  $z = Z$ . The tristimulus can be converted into  $R_0$ ,  $G_0$  and  $B_0$  values by using the function “xyz2rgb” issued by MathWorks, then the color of any point in CIE chromatic diagram can be defined by normalized  $R_0$ ,  $G_0$ ,  $B_0$  values.



## S6. Design and fabrication of the color printing devices

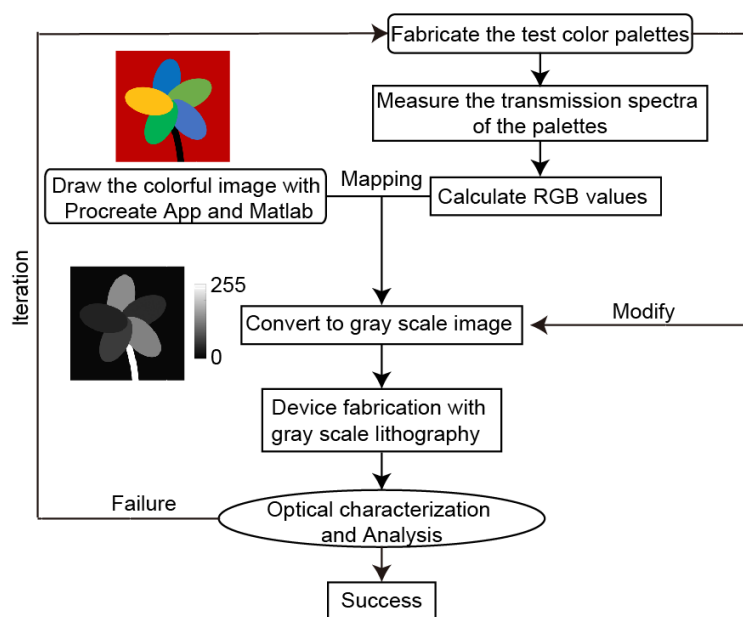


**Fig. S7** The flowchart of design and fabrication of the color printing device.

Firstly, the color palettes based on the concept of the Fabry-Perot cavities and the laser grayscale lithography technique were fabricated. By measuring the transmission spectra and calculate the CIE values, we have a library of F-P cavities, which can be used for drawing the colorful image with Procreate App. The colorful image is then converted to a grayscale image by a self-developed Matlab code. The grayscale image is then imported into the Heidelberg Instruments DLW 66<sup>+</sup> to engrave the photoresist layer, which is sitting on the silver mirror. After depositing the second silver mirror and a SiO<sub>2</sub> encapsulation layer on the patterned photoresist layer, the optical properties of the color printing device will be characterized. In the iterative step, a test color palette will be fabricated. The colors of the new palettes could further guide the optimization of the design and fabrication process.

*Fabrication of the Fabry-Perot cavities:* The Fabry-Perot cavities were fabricated on the glass substrates which were cleaned in ultrasonic baths of acetone, isopropyl alcohol and deionized water in sequence. Then, the electron beam evaporation technique was used to deposit a 30 nm thick silver film on the glass substrate. The pressure of  $\sim 6\text{e-}6$  mbar in the chamber of the electron beam evaporator (HHV AUTO 500) was kept during the thin film deposition process. The evaporation rate is about  $0.84 \text{ \AA s}^{-1}$ . After that, the grayscale photoresist AZ4562 from Microchemicals GmbH was spin-coated on top of the silver film. After baking at temperature of 100°C for 3 minutes, the thickness of the photoresist film is about 150 nm.

The laser grayscale photolithography process was carried out by using the Direct laser writing system DWL 66+ from Heidelberg Instruments (laser wavelength: 405 nm). The grayscale pattern in the photoresist layer can be achieved by controlling the exposure dose ( $< 22 \mu\text{W} \mu\text{m}^{-2}$ ) of each pixel. The exposed photoresist was then developed by a diluent AZ400K solution (Microchemicals GmbH). The photoresist with three dimensional profiles are formed. Finally, the second silver film with thickness of 30 nm thick was deposited on the photoresist layer to form the pixelated Fabry-Perot cavities. To avoid the oxidation of the top silver film, a 20 nm thick  $\text{SiO}_2$  encapsulation layer was coated on the top of the silver layer by using electron beam evaporation method. The deposition rate of the  $\text{SiO}_2$  layer is  $\sim 0.625 \text{ \AA s}^{-1}$ . The thickness of the silver, photoresist and  $\text{SiO}_2$  films were measured through the spectroscopic ellipsometer (Horiba TF-UVISEL). By measuring the transmission properties of the cavities, we are able to correlate the precise thickness of the PR layer and the corresponding exposure doses.

## S7. Color filter arrays based on the pixelated Fabry-Perot cavities

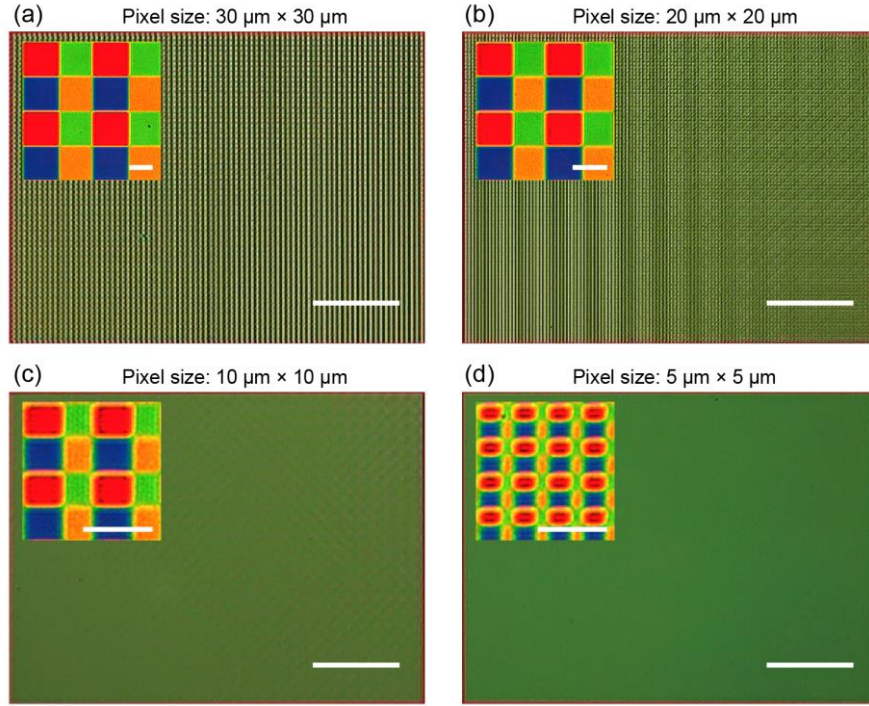


**Fig. S8** Photos of the color filter arrays. The size of the color filter arrays is  $3.6 \text{ mm} \times 4.8 \text{ mm}$ , which is same as that of a 1/3-inch CMOS image sensor. In each pattern, the unit cell consists of  $2 \times 2$  pixels. The four pixels working at Red, Yellow, Green and Blue wavelengths. (a)–(d) The pixel size are  $30 \mu\text{m} \times 30 \mu\text{m}$ ,  $20 \mu\text{m} \times 20 \mu\text{m}$ ,  $10 \mu\text{m} \times 10 \mu\text{m}$  and  $5 \mu\text{m} \times 5 \mu\text{m}$ , respectively. Scale bars: 1 mm. The insert pictures are taken by a microscopy, and the scale bars are  $20 \mu\text{m}$ .

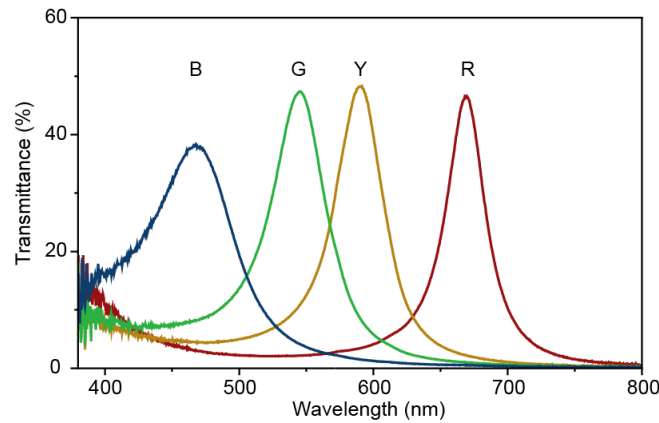


**Fig. S9** Transmission spectra of the four kinds of Fabry-Perot cavities. The transmission peaks of for color filters are 669 nm (Red), 591 nm (Yellow), 545 nm (Green) and 468 nm (Blue), respectively.